American Journal of Analytical Chemistry, 2016, 7, 203-209
Published Online February 2016 in SciRes. http://www.scirp.org/journal/ajac
http://dx.doi.org/10.4236/ajac.2016.72017

Preparation and Structural Properties of $ZnAl_xFe_{2-x}O_4$ Spinel Oxide

Shahzad Hossain[1,2*], Goutam Dev[3], Mst. Sanjida Aktar[1], Muhammad Kamrul Hasan[3], A. K. M. Zakaria[1], Tapash Kumar Datta[1], Imtiaz Kamal[1], Sk. Md. Yunus[1], Md. Habibul Ahsan[3], Abul Kalam Azad[2]

[1]Institute of Nuclear Science & Technology, Bangladesh Atomic Energy Commission, Dhaka, Bangladesh
[2]Faculty of Integrated Technologies, Universiti Brunei Darussalam, Gadong, Brunei Darussalam
[3]Department of Physics, Shahjalal University of Science and Technology, Sylhet, Bangladesh
Email: *shahzad_baec@yahoo.com

Received 19 January 2016; accepted 20 February 2016; published 23 February 2016

Abstract

The $ZnAl_xFe_{2-x}O_4$ (x = 0.0, 0.2 and 0.4) spinel ferrites were prepared by the conventional solid state reaction in air at 1350˚C. The X-ray diffraction of all the three samples showed sharp Bragg peaks indicating the formation of a single phase spinel structure. The lattice parameters of the samples were determined from the X-ray diffraction data using the Nelson-Riley extrapolation method. The lattice parameters, cation distribution and oxygen position parameters have also been determined by refining the data by the Rietveld method. Rietveld refinement of the XRD data reveals all the samples to possess cubic symmetry corresponding to the space group Fd3m. Lattice parameters were found to decrease with increasing Al concentration, *i.e.* 8.4322, 8.4002, and 8.3984 Å for x = 0.0, 0.2 and 0.4, respectively.

Keywords

Polycrystalline Ferrite, X-Ray Diffraction, Spinel Ferrite, Rietveld Refinement, Space Group Fd3m, Lattice Parameter

1. Introduction

Spinel oxides have gained much technological importance because of their high resistance and exciting magnetic characteristics. The general chemical formula of the spinel ferrites is AB_2O_4, where A is a divalent metal ion (cation) and B is a trivalent metal ion (cation). In magnetically diluted ferrites the ferric ions are distributed

*Corresponding author.

How to cite this paper: Hossain, S., Dev, G., Aktar, M.S., Hasan, M.K., Zakaria, A.K.M., Datta, T.K., Kamal, I., Yunus, S.M., Ahsan, M.H. and Azad, A.K. (2016) Preparation and Structural Properties of $ZnAl_xFe_{2-x}O_4$ Spinel Oxide. *American Journal of Analytical Chemistry*, **7**, 203-209. http://dx.doi.org/10.4236/ajac.2016.72017

among octahedral B site and tetrahedral A site lattice positions. Ferrite is known to be a spinel oxide consisting of a cubic close-packed arrangement of anions (oxygen ions) with one half of the octahedral interstices (B sites) and one-eighth of the tetrahedral interstices (A sites) occupied with cations. Ferrites have many applications because of their high resistivity and permeability. Ferrite cores are used in electronic inductors, transformers, electromagnets, radio engineering and computer technology [1]. Most common radio magnets, including those used in loudspeakers, are ferrite magnets. It is a common magnetic material for electromagnetic instrument pickups because of low price and relatively high output. The interest of studying ferrites with different compositions using different techniques is due to their diversified uses [2]-[6]. Crystallographic methods depend on the analysis of the diffraction patterns of a sample obtained from X-ray or neutron diffraction. Diffraction method, especially X-ray diffraction, is widely used in materials science [7]-[13]. The X-ray or neutron diffraction is used to identify the patterns which are present in a particular material, and thus which compounds are present [14] [15].

Because of their high opacity, zinc ferrites can be used as pigments, especially in applications requiring heat stability. For example, zinc ferrite prepared from iron oxide can be used as a substitute for applications in temperatures above 350˚F (177˚C) [16]. When added to high corrosion-resistant coatings, the corrosion protection increases with an increase in the concentration of zinc ferrite [17]. A recent investigation shows that the zinc ferrite, which is paramagnetic in the bulk form, becomes ferrimagnetic in nanocrystalline thin film format [18]. A large room temperature magnetization and narrow ferromagnetic resonance line width have been achieved by controlling thin films growth conditions [19].

In this research aluminum doped zinc ferrite, $ZnAl_xFe_{2-x}O_4$ with x = 0.0, 0.2 and 0.4 (ZAF) were prepared to investigate the effect of Al on zinc ferrite and how the lattice parameters change with Al doping and was characterized by X-ray diffraction. Lattice parameters of all the samples have been determined by the Nelson-Riley function and compared with the values obtained from XRD. Density, porosity, lattice parameters, oxygen positions and cation distributions have been determined using X-ray diffraction data.

2. Experimental

2.1. Synthesis of $ZnAl_xFe_{2-x}O_4$ (ZAF)

$ZnAl_xFe_{2-x}O_4$ (x = 0.0, 0.2, 0.4) were prepared by the solid state reaction. Powder of ZnO (99% pure), Al_2O_3 (99% pure), Fe_2O_3 (99% pure) were used as initial chemicals in precise stoichiometric ratios. The chemicals were weighed individually using a digital micro balance and then thoroughly mixed in an agate mortar for two hours of each sample. Then the samples were milled intimately in a stainless steel ball-milling for about 6 hours. For fine mixing of the ingredients, a small amount of distilled water was used. Then the mixtures were dried on a magnetic heater and then calcinated in an alumina crucible at 800˚C in air for 8 hours inside a muffle furnace to homogenize the product. Little amount of polyvinyl alcohol (PVA) was added to each dried powder as binder and was again closely grinded. The powders were then pressed into pellets of 13 mm dia using a hydraulic press with 5 tons pressure. All pellets were slightly brick reddish in color and were finally sintered at 1350˚C for 6 hours in air with the rate of 5˚C/min and then converted into powder again for X-ray diffraction experiment.

2.2. Structural Analysis

The X-ray diffraction experiments were performed on all the samples using X' Pert PRO XRD system (Manufacturer: PANalytical, Frankfurt, Germany) with $CuK_{\alpha 1}$ radiation of wavelength λ = 1.54056 Å in the angular range of 2θ = 15˚ to 90˚ with a step size of 0.025˚ at room temperature. The X-ray diffraction patterns for all the samples have been indexed using the indexing program TREOR90 [20]. The lattice constants, oxygen position parameters and cation distributions been determined precisely by using the Rietveld refinement [21] program RIETAN-2000 [22].

3. Results and Discussion

3.1. XRD Pattern Analysis

Figure 1 shows the Rietveld analysis profile of X-ray diffraction data of $ZnAl_{0.2}Fe_{1.8}O_4$ at room temperature.

Rietveld analysis of the X-ray diffraction patterns confirms the single phase spinel structure for all the three samples. It was found that (311) Bragg reflection has the highest intensity for all samples. The crystal structure of spinel oxide is defined by three crystallographic parameters, namely the lattice constant (a_0), oxygen position

parameter (u) and cation distribution on the A and B sites.

The spinel structure exhibits the symmetry of the space group Fd3m and this space group has been used in the data refinement process for generating the calculated diffraction profile. The occupation numbers of cations at A and B sites and other structural parameters have been obtained from the basis of the best fit to the observed data. It is evident from the agreement factors that the observed and calculated intensities are quite satisfactory.

In the refinement process lattice constants, oxygen position parameters and cation distribution have been determined and presented in **Table 1**. In the table we see that the lattice constants decrease with the increase of Al contents. This is due to the effect of the size or radius of the aluminum atom in comparison with the iron (iron is bigger than the aluminum).

The agreement factors (R-factors) and χ^2 are the indicators of the goodness of fit of the refinement parameters. The values of R-factors (%) and χ^2 obtained from the Rietveld refinement of the X-ray data by using the program RIETAN-2000 are given in **Table 2**. The goodness of fits (χ^2) is increased with the increasing of aluminum and may be due to the ratio or number of aluminum atoms increased or decreasing of iron atoms from the zinc ferrite. The profile R factor, weighted R factor is increased with the increasing of aluminum, on the other hand the expected R factor decreased with the increasing of it.

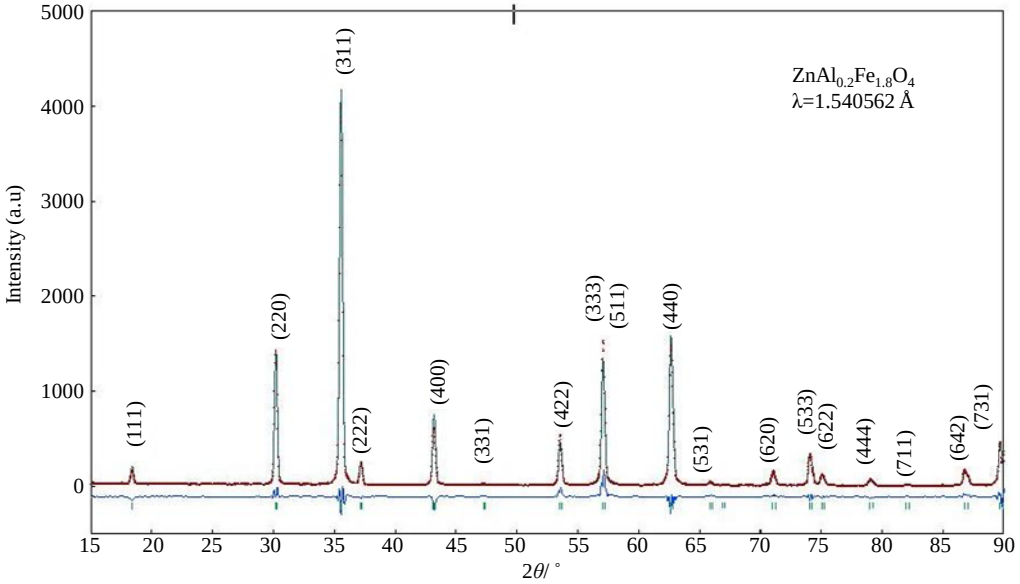

Figure 1. Reitvelt analysis profile of XRD pattern of spinel oxide $ZnAl_{0.2}Fe_{1.8}O_4$ at room temperature.

Table 1. Lattice parameters, oxygen position parameters and cation distribution of the spinel oxides ZAF.

Sample	Lattice constant a_o (Å)	Oxygen parameter u (o)	Cation distribution	
			Tetrahedral (8a) site	Octahedral (16d) site
$ZnFe_2O_4$	8.4322	0.376606	$(Fe_{0.5}Zn_{0.5})_A$	$(Fe_{1.5}Zn_{0.5})_B$
$ZnAl_{0.2}Fe_{1.8}O_4$	8.4002	0.381892	$(Fe_{0.4}Zn_{0.6})_A$	$(Fe_{1.4}Zn_{0.4}Al_{0.2})_B$
$ZnAl_{0.4}Fe_{1.6}O_4$	8.3984	0.384244	$(Fe_{0.25}Zn_{0.75})_A$	$(Fe_{1.35}Zn_{0.25}Al_{0.4})_B$

Table 2. Goodness of fit, different R factors of the spinel oxides ZAF.

Sample	Goodness of fit (χ^2)	Profile R factor (R_p)	Weighted R factor (R_{wP})	Bragg R factor (R_I)	Expected R factor (R_E)
$ZnFe_2O_4$	0.9541	8.31	11.00	6.80	11.53
$ZnAl_{0.2}Fe_{1.8}O_4$	0.9797	8.55	11.24	6.80	11.36
$ZnAl_{0.4}Fe_{1.6}O_4$	0.9984	8.86	11.46	6.84	11.22

The site occupancies of different cations have been determined by varying them within the stoichiometric constraint. The occupation of oxygen ions for all the samples have been kept fixed during the refinement.

The positions of the several diffraction peaks, d-spacing, lattice parameters, N-R functions, relative intensities and corresponding Miller indices of $ZnAl_{0.4}Fe_{1.6}O_4$ are given in **Table 3**.

3.2. Lattice Parameters

Lattice parameter decreases with Al doping. The decrease in lattice parameter is due to the smaller ionic radius of Al in comparison to Fe. The change in lattice parameters with doping follows the Vegard's law with a very small deviation for x = 0.2 composition. **Figure 2** shows the plot of lattice parameter versus doping concentration. Nelson-Riley [23] function was calculated to find the greater range of linearity. The calculated values of Nelson-Riley (N-R) functions are plotted against the lattice parameters in **Figures 3-5** for the three composition of x = 0.0, 0.2 and 0.4 respectively.

3.3. Bulk Density

The bulk density (ρ_B) has been calculated by using the usual mass volume ratio; X-ray density (ρ_x) by using molecular weight, Avogadro's constant & lattice constants and porosity (ρ) has been calculated by using both bulk density and X-ray density.

The calculated bulk density, X-ray density and porosity of the three samples are given in **Table 4**. The bulk density increases with the increases of aluminum, due to the smaller size of aluminum which create less porous inside the material around the spheres of aluminum.

Table 3. Bragg intensities of different (h k l) values of spinel oxides $ZnAl_{0.4}Fe_{1.6}O_4$ at room temperature.

(h k l)	2θ (degree)	d-spacing	Lattice Parameters a (Å)	N-R function	Relative intensity (%)
(111)	18.3994	4.82208	8.35208756	3.100445775	3.27
(220)	30.1921	2.96016	8.37259684	1.820498838	36.39
(311)	35.5511	2.52527	8.37537308	1.510654959	100
(222)	37.1896	2.41769	8.37512383	1.432739436	4.73
(400)	43.1925	2.09457	8.37828000	1.194444386	16.19
(422)	53.5527	1.71126	8.38342763	0.899484348	13.49
(511)	57.0834	1.61352	8.38409586	0.821086664	31.81
(440)	62.6696	1.48246	8.38606015	0.713090596	48.06

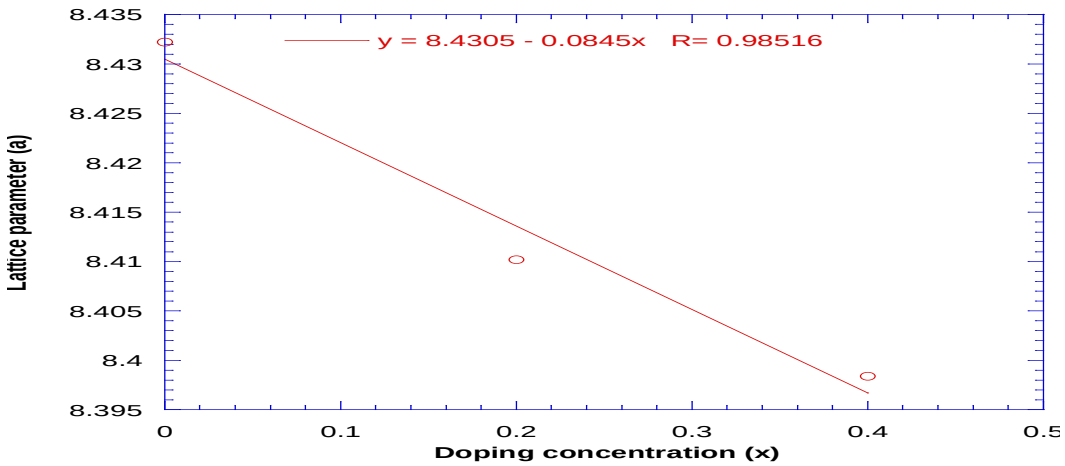

Figure 2. Lattice parameters versus doping concentration of spinel oxide $ZnAl_xFe_{2-x}O_4$ at room temperature.

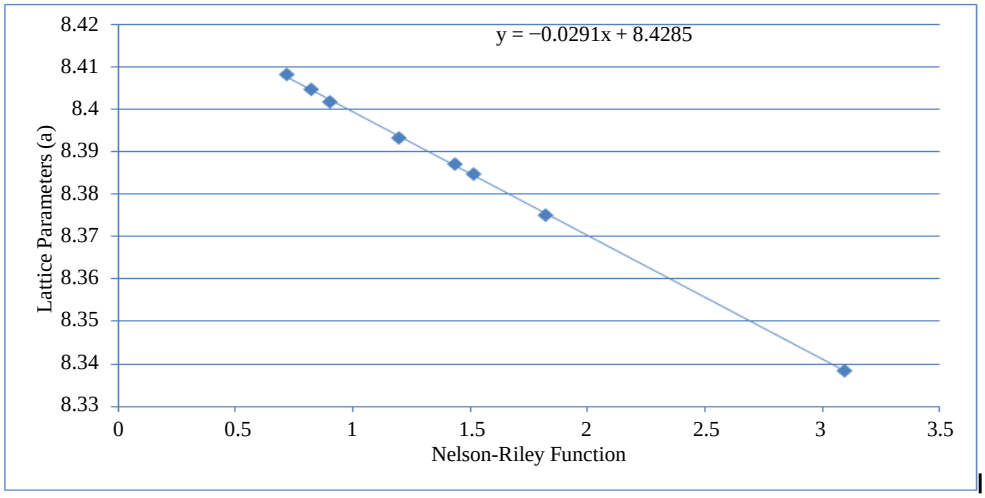

Figure 3. Lattice parameters versus Nelson-Riley function of $ZnFe_2O_4$.

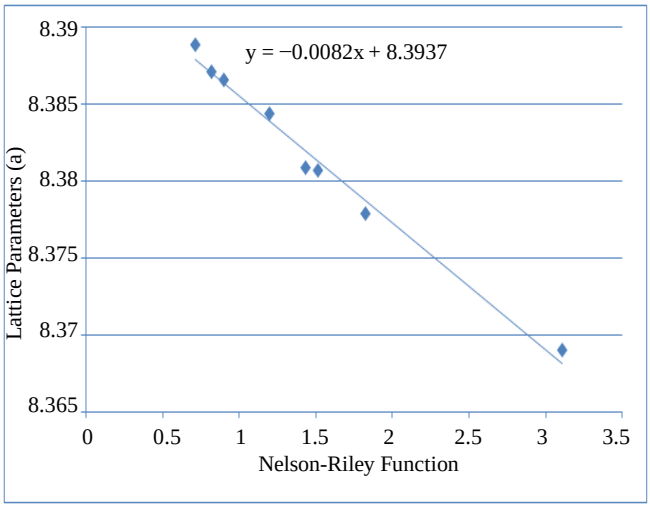

Figure 4. Lattice parameters versus Nelson-Riley functions of $ZnAl_{0.2}Fe_{1.8}O_4$.

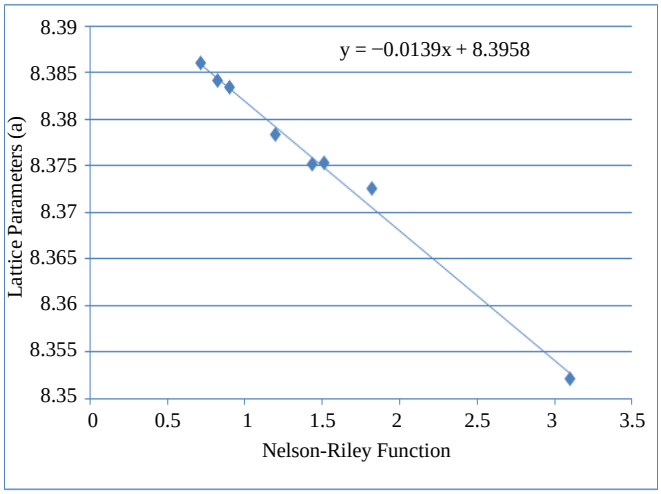

Figure 5. Lattice parameters versus Nelson-Riley functions of $ZnAl_{0.4}Fe_{1.6}O_4$.

Table 4. Buck density, X-ray density and porosity of spinel oxides ZAF at room temperature.

Sample	Bulk density ρ_B (g/cm^3)	X-ray density ρ_x (g/cm^3)	Porosity ρ (in %)
$ZnFe_2O_4$	4.5938	5.3948	12.993
$ZnAl_{0.2}Fe_{1.8}O_4$	4.6843	5.3260	11.926
$ZnAl_{0.4}Fe_{1.6}O_4$	4.7869	5.1987	10.920

4. Conclusion

The X-ray diffraction patterns demonstrate that the polycrystalline ferrites prepared in the solid state ceramic method are of single phase cubic spinel structure. The lattice parameters of the samples decrease with the increase of Al concentration. The values of different crystallographic parameters and cation distributions are obtained the best fit from the analysis of the X-ray diffraction data. In $ZnFe_2O_4$: Zn^{2+} ions were distributed over both tetrahedral (A) site and octahedral (B) sites; 50% of the Zn^{2+} ions were occupied the tetrahedral (A) site and the rest of its (50%) at octahedral (B) site; 25% of the Fe^{3+} ions were occupied tetrahedral (A) site and rest (75%) at the octahedral (B). In $ZnAl_{0.2}Fe_{1.8}O_4$: 100% of Al^{3+} ions were occupied the octahedral (B) site; 60% of the Zn^{2+} ions were occupied the tetrahedral (A) site and the rest (40%) at the octahedral (B); 22.22% of the Fe^{3+} ions were occupied the tetrahedral (A) site and rest of it (77.78%) at the octahedral (B). In $ZnAl_{0.4}Fe_{1.6}O_4$: 100% of Al^{3+} ions were occupied the octahedral (B) site; 75% of the Zn^{2+} ions were occupied the tetrahedral (A) site and the rest (25%) at octahedral (B); 15.62% of the Fe^{3+} ions were occupied the tetrahedral (A) site and rest (84.38%) at the octahedral (B). The bulk density and X-ray density of all the samples found that the individual specimen showed good consistency between themselves irrespective of aluminum contents.

Acknowledgements

The authors are thankful to the Institute of Nuclear Science & Technology (INST) and Atomic Energy Centre Dhaka (AECD) of Bangladesh Atomic Energy Commission (BAEC) for supporting the facilities for this research work done successfully.

References

[1] Oliver, S.A., Harris, V.G., Hamdeh, H.H. and Ho, J.C. (2000) Large Zinc Cation Occupancy of Octahedral Sites in Mechanically Activated Zinc Ferrite Powders. *Applied Physics Letters*, **76**, 2761-2763. http://dx.doi.org/10.1063/1.126467

[2] Ghatage, S.A., Patil, S.A. and Paranjpe, S.K. (1996) Neutron Diffraction Study of Chromium Substituted Nickel Ferrite. *Solid State Communications*, **98**, 885-888. http://dx.doi.org/10.1016/0038-1098(96)00036-1

[3] Corliss, L.M., Hastings, J.M. and Brockman, F.G. (1953) A Neutron Diffraction Study of Magnesium Ferrite. *Physical Review*, **90**, 1013-1018. http://dx.doi.org/10.1103/PhysRev.90.1013

[4] Murthy, N.S.S., Natera, M.G., Youssef, S.I., Begum, R.J. and Srivastava, C.M. (1969) Yafet-Kittel Angles in Zinc-Nickel Ferrites. *Physical Review*, **181**, 969-977. http://dx.doi.org/10.1103/PhysRev.181.969

[5] Yunus, S.M., Asgar, M.A. and Ahmed, F.U. (2000) Neutron Diffraction Study of Magnetic Ordering in the Spinel Oxide $Co_xMn_{1-x}Al_{2x}Fe_{2-2x}O_4$. *Journal of Alloys and Compounds*, **298**, 9-17. http://dx.doi.org/10.1016/S0925-8388(99)00613-1

[6] Happel, H. and Hoenig, H.E. (1973) The Specific Heat Jump of Superconducting $La_{1-x}Tb_xAl_2$ Related to Crystal Electric Field Splitting of the Tb^{3+} Levels. *Solid State Communications*, **13**, 1641-1643. http://dx.doi.org/10.1016/0038-1098(73)90256-1

[7] Wills, B.T.M. (1970) Thermal Neutron Diffraction. Oxford University Press, Oxford.

[8] Wills, B.T.M. (1973) Chemical Applications of Thermal Neutron Scattering. Oxford University Press, Oxford.

[9] Cullity, B.D. (1978) Elements of X-ray Diffraction. 2nd Edition, Addison-Wesley, Boston, MA.

[10] Zakaria, A.K.M., Asgar, M.A., Eriksson, S.-G., Ahmed, F.U., Yunus, S.M., Azad, A.K. and Rundlöf, H. (2003) Preparation of Zn Substituted Ni–Fe–Cr Ferrites and Study of the Crystal Structure by Neutron Diffraction. *Materials Letters*, **57**, 4243-4250. http://dx.doi.org/10.1016/S0167-577X(03)00298-2

[11] Azad, A.K., Eriksson, S.-G., Yunus, S.M., Eriksen, J. and Rundlöf, H. (2003) Synthesis, Cation Distribution and Crystal Structure of the Spinel Type Solid Solution $Ga_xCoFe_{1-x}CrO_4$ ($0 \leq x \leq 1$). *Physics B*: *Condensed Matter*, **327**, 1-8. http://dx.doi.org/10.1016/S0921-4526(02)01455-2

[12] Zakaria, A.K.M., Asgar, M.A., Ahmed, F.U., Azad, A.K., Yunus, S.M., Paranjpe, S.K. and Das, A. (2002) Studies of $Mn_{0.5}Cr_{0.5}Fe_2O_4$ Ferrite by Neutron Diffraction at Different Temperatures in the Range 768 > T > 13K. *Indian Journal of Pure and Applied Physics*, **40**, 46-53.

[13] Hossain, S., Hasan, M.K., Yunus, S.M., Zakaria, A.K.M., Datta, T.K. and Azad, A.K. (2015) Synthesis and Investigation of the Structural Properties of Al^{3+} Doped Mg Ferrites. *Applied Mechanics and Materials*, **789-790**, 48-52. http://dx.doi.org/10.4028/www.scientific.net/AMM.789-790.48

[14] Snigirev, A., Bjeoumikhov, A., Erko, A., Snigireva, I., Grigoriev, M., Yunkin, V., Erkob, M. and Bjeoumikhovae, S. (2007) Two-Step Hard X-ray Focusing Combining Fresnel Zone Plate and Single-Bounce Ellipsoidal Capillary. *Journal of Synchrotron Radiation*, **14**, 326-330. http://dx.doi.org/10.1107/S0909049507025174

[15] Clegg, W. (1998) Crystal Structure Determination (Oxford Chemistry Primer). Oxford University Press, Oxford, 84 p.

[16] Zinc Ferrites: Nubiola.com, Retrieved 25 March 2010. https://en.wikipedia.org/wiki/Zinc_ferrite

[17] Zinc Ferrite: Hoover Color Corporation, Retrieved 25 March 2010. http://www.hoovercolor.com/products/pigments/zincferrite/

[18] Ayana, Y.M.A., El-Sawy, S.M. and Salah, S.H. (1997) Zinc-Ferrite Pigment for Corrosion Protection. *Anti-Corrosion Methods and Materials*, **44**, 381-388. http://dx.doi.org/10.1108/00035599710367681

[19] Bohra, M., Prasad, S., Kumar, N., Misra, D.S., Sahoo, S.C., Venkataramani, N. and Krishnan, R. (2006) Large Room Temperature Magnetization in Nanocrystalline Zinc Ferrite Thin Films. *Applied Physics Letters*, **88**, 262506-262506-3. http://dx.doi.org/10.1063/1.2217253

[20] Werner, P.E., Eriksson, L. and Westdahl, M. (1985) TREOR, A Semi-Exhaustive Trial-and-Error Powder Indexing Program for All Symmetries. *Journal of Applied Crystallography*, **18**, 367-370. http://dx.doi.org/10.1107/S0021889885010512

[21] Riteveld, H.M. (1967) Line Profiles of Neutron Powder-Diffraction Peaks for Structure Refinement. *Acta Crystalloghraphica*, **22**, 151. http://dx.doi.org/10.1107/s0365110x67000234

[22] Izumi, F. and Ikeda, T. (2000) A Rietveld-Analysis Programm RIETAN-98 and Its Applications to Zeolites. *Materials Science Forum*, **321-324**, 198-205. http://dx.doi.org/10.4028/www.scientific.net/MSF.321-324.198

[23] Nelson, J.B. and Riley, D.P. (1945) An Experimental Investigation of Extrapolation Methods in the Derivation of Accurate Unit-Cell Dimensions of Crystals. *Proceedings of Physical Society*, **57**, 160-177. http://dx.doi.org/10.1088/0959-5309/57/3/302